2008

Novel Magnetic Photonic Crystal Structures for Magnetic Field Sensors and Visualizers

Mikhail Vasiliev
Edith Cowan University

Viatcheslav A. Kotov
Institute of Microtechnology-Spin MT, Moscow, Russia

Kamal E. Alameh
Edith Cowan University

Vladimir I. Belotelov
Institute of Microtechnology-Spin MT, Moscow, Russia

Anatoly K. Zvezdin
Institute of Microtechnology-Spin MT, Moscow, Russia

10.1109/TMAG.2007.914675

This article was originally published as: Vasiliev, M. , Kotov, V.A., Alameh, K.E. , Belotelov, V.I., & Zvezdin, A.K. (2008). Novel Magnetic Photonic Crystal Structures for Magnetic Field Sensors and Visualizers. IEEE Transactions on Magnetics, 44(3), 323-328. Original article available here

Novel Magnetic Photonic Crystal Structures for Magnetic Field Sensors and Visualizers

Mikhail Vasiliev[1], Viatcheslav Alekseevich Kotov[2], Kamal E. Alameh[1], Vladimir I. Belotelov[2], and Anatoly Konstantinovich Zvezdin[2]

[1]Centre of Excellence for MicroPhotonic Systems, Electron Science Research Institute, Edith Cowan University, Joondalup, WA 6027, Australia
[2]Institute of Microtechnology-Spin MT, 119311 Moscow, Russia

Optimized one-dimensional (1-D) magnetophotonic crystals greatly increase the sensitivity of magnetooptical sensors, which are widely used in magnetooptical imaging to observe the magnetic domain patterns in magnetic materials, to observe the vortex states in superconductors, to detect small bits in magnetooptical recording media, to visualize defects in ferromagnetic objects, and to measure the value and spatial distribution of stray magnetic fields. This paper examines the properties of such devices operating in the optimized reflection (doubled Faraday rotation) mode and discusses the use of 1-D magnetophotonic crystals as sensors.

Index Terms—**Magnetic domains, magnetic photonic crystals, magnetooptical magnetic field sensors.**

I. Introduction

MAGNETOOPTICAL (MO) imaging and sensing devices utilizing Bi-substituted iron garnet films are widely used to examine the spatial distribution of magnetic fields produced by magnetized objects [1]–[5], to study the vortex matter in high-temperature superconductors [6], and as current sensors [7]. Depending on the properties of the objects under study, the sensing films with in-plane, inclined, and perpendicular orientation of the magnetization vector with respect to the film plane are used [1]. The in-plane magnetized films usually provide more flexibility for the characterization of objects under investigation. At the same time, films possessing the maze-like domain structure and small saturating magnetic fields are more suitable for detecting localized magnetic defects in ferromagnetic samples [3]. The films with inclined magnetization direction are rarely mentioned, nevertheless, due to their excellent linearity, they are very suitable in magnetic field measurement systems. In this paper, we discuss the ways of optimizing the properties of MO films and photonic nanostructures with perpendicular magnetization for use in magnetic field visualizers and sensors based on the changes in the magnetic domain structure under the influence of external magnetic fields.

A typical configuration of a MO sensor is shown in Fig. 1. In this case, a liquid phase epitaxial (LPE) Bi-substituted iron garnet film with a typical thickness from 2 to 5 μm coated with a thin aluminum reflecting layer is placed on top of the sample. A polarized light beam passes through the sensing film, is reflected at the bottom, and rotates the polarization vector in proportion to the vertical component of the magnetic moment of the sensing film. In the usual case, double Faraday rotation of the sensing film appears to be much higher then its Kerr rotation angle originating from the reflection off the upper surface

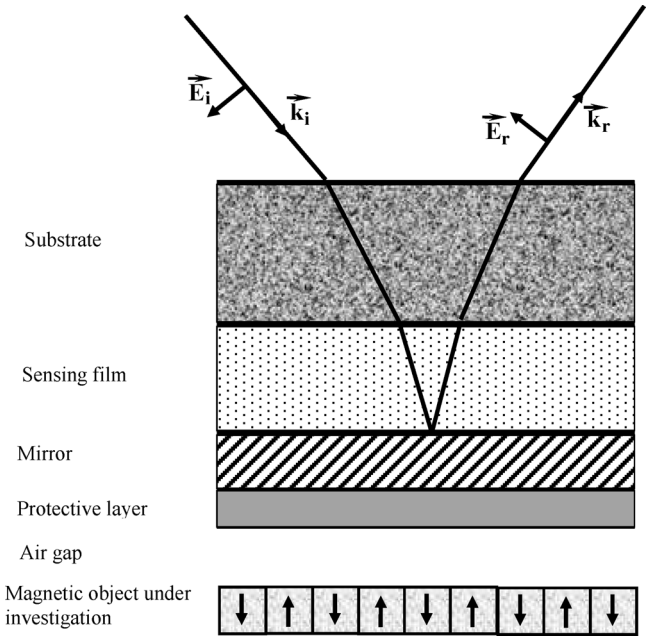

Fig. 1. Operation of MO thin film sensor in reflection mode.

of the film. In films with in-plane and inclined direction of the magnetization the magnetic stray field produced by the sample rotates the local magnetic moment of the sensing film in either the "up" or "down" direction. If a sensor is based on a film with the perpendicular direction of the magnetization with respect to the film plane, such a film possesses a maze-like or stripe domain structure.

To characterize the performance of a MO sensor with in-plane magnetization, its photo-response (P/R) characteristic is used [4]:

$$P/R = \frac{I_{\text{out}}}{I_{\text{inc}}} = \frac{1}{2}\left[1 + \sin(2\Phi_F h \cos\theta)\right]\exp(-2\alpha h) \quad (1)$$

where I_{inc} and I_{out} are the incident (plane-polarized) optical intensity and output optical intensity detected after passing through the analyzer oriented at 45° with respect to the input polarization plane, respectively, Φ_F and h are the specific

Digital Object Identifier 10.1109/TMAG.2007.914675

Color versions of one or more of the figures in this paper are available online at http://ieeexplore.ieee.org.

Faraday rotation of the sensing film and the film thickness, and α is the absorption coefficient of the film material. The term $\cos(\theta)$ is equal to B_n/B_s, where B_n is the measured component of magnetic induction applied in the direction perpendicular to the film plane, B_s is the magnetic induction necessary to saturate the magnetization in the film along the film normal, and θ is the angle between the film normal and the magnetization vector $\mathbf{M}$. The term $\exp(-2\alpha h)$ describes the absorption of light during its propagation through the film in both directions.

The dynamic range of an MO sensor is determined by the saturation induction B_s which depends on the film composition and can be varied from 10 to 2000 Oe. On the other hand, the sensitivity S is given by [4]

$$S = \left.\frac{d(P/R)}{dB_n}\right|_{B_n=0} = \frac{\Phi_F h}{B_s}. \tag{2}$$

Thus, the higher the sensitivity, the lower the dynamic range is, and vice versa. To obtain high sensitivity, B_s must be small and Φ_F must be large.

Another important parameter of the sensor is the spatial resolution of the film determined by its magnetic properties, thickness, and also the distance between the reflecting mirror and the surface of the sample under investigation. The value of the spatial resolution (its order of magnitude) is determined by the sum of the thicknesses of the film, the mirror, the protective layer, and the air gap between the protective layer and the object under investigation.

The approach of using magnetic photonic crystals (MPC) provides an opportunity to increase the Faraday rotation angle of the MPC by about an order of magnitude in the visible spectral region even with a rather high absorption level of about 1000 cm^{-1} present in the LPE iron garnet films in the spectral region from 540 to 650 nm. Of course, in the infrared spectral region, where the absorption coefficient drops to the level of about 10^{-3} cm^{-1} or smaller, the growth of the sensitivity will be much higher, but at the same time, the spatial resolution is diminished substantially because the optimal thickness of the sensing film increased essentially in this case.

The reflection mode operation of one-dimensional (1-D) magnetophotonic crystals for use in film-based magnetooptical isolator devices was considered in [8], [9]. The authors discussed the case of nonabsorbing MO materials and described a symmetrical MPC structure of the type (SiO2/Ta2O5)k/Bi:YIG/(Ta2O5/SiO2)k/R with a reflecting layer R [9]. The performance characteristics for three cases of the reflection layer R, namely, a single aluminum layer ($R = \mathrm{Al}$), a dielectric multilayer film [$R = (\mathrm{Ta_2O_5/SiO_2})^{\mathrm{n}}$], and their combinations [$R = (\mathrm{Ta_2O_5/SiO_2})^{\mathrm{n}}/\mathrm{Al}$] were examined. Here, we extend the analysis of the reflection-mode MPC operation by considering the case of using MPC structures optimized for magnetic field sensors and sensors working in the visible spectral region, where it is necessary to enable reliable device operation in the presence of significant material absorption within magnetic layers. We also discuss the properties of several generic types of MPC structures suitable for this application and the approaches for optimizing the sensitivity of sensors by controlling the magnetic properties of MPC constituents via the design of the material composition and layer geometry.

II. Sensitivity of MPC Sensors

As was mentioned in the introduction, in a number of practical measurement situations sensing films with maze-type domain structure are desired. This is due to their suitability for the detection of small localized magnetic defects (for example, cavities inside ferromagnetic objects). The MPC sensor possessing the domain structure can provide an increase in the sensitivity of MO sensors of two orders of magnitude, depending on the absorption coefficient of the magnetic and nonmagnetic media in the desired spectral region and the magnetic and magnetooptical properties of the materials used. As we can see from (2), the sensitivity of a single-layer film is determined by its Faraday rotation and the value of the saturation field at which the domain structure disappears ($S = \Phi_F h/B_s$). We can separate the sensor sensitivity described by (2) into two contributions: the first one being due to Faraday rotation, and the second is due to the saturation field B_s.

The Faraday rotation contribution to the full sensitivity can be increased by a factor of about 2 compared with usually used sensing films by optimizing the composition of the film, and further by a factor of up to about 10 (in the visible region) or higher (in the infrared) due to using the MPC structure. Obviously, this "gain" in the Faraday rotation is strongly dependent on the absorption coefficient of the magnetic material.

The saturation field can be reduced substantially by optimizing the thicknesses of individual magnetic layers within MPC. In the case of a single-layer magnetooptical sensor, the attainable values of Faraday rotation and saturation fields are interrelated via the composition and magnetic properties of the magnetooptical material. In order to increase the specific Faraday rotation of the material, the composition of LPE film with the ultimate content of Bi nonsubstituted in iron sublattices (for example $(\mathrm{BiSmLu})_3\mathrm{Fe_5O_{12}}$) with values of the saturation magnetization $4\pi M_s$ of about 1700 Oe must be used.

The Sm and Lu ions are introduced here to provide the necessary value of the uniaxial magnetic anisotropy and to achieve the stripe- or maze-like domain structure.

In the usual case of a single-layer film sensor, for an optimal thickness of the sensor film (typical thickness of the films is between 2 and 5 μm), the saturation field is in the range of 500–1000 Oe, depending on the film thickness and composition. As a result, attaining the ultimate magnetooptical properties leads to a significant drop in the magnetic sensitivity.

In an MPC structure intended for operation in the green spectral region, the typical thickness of the individual magnetooptical layers is near 50 nm, and there is a possibility to change this value within some range to optimize the saturation field and the domain size in the individual layers of the MPC structure. Of course, we must then also change the thickness of the surrounding (nonmagnetic) layers to attain a necessary period of MPC structure determining the operational wavelength of the MPC.

The spatial resolution of the sensor based on the use of the domain structure is determined by the width of the magnetic

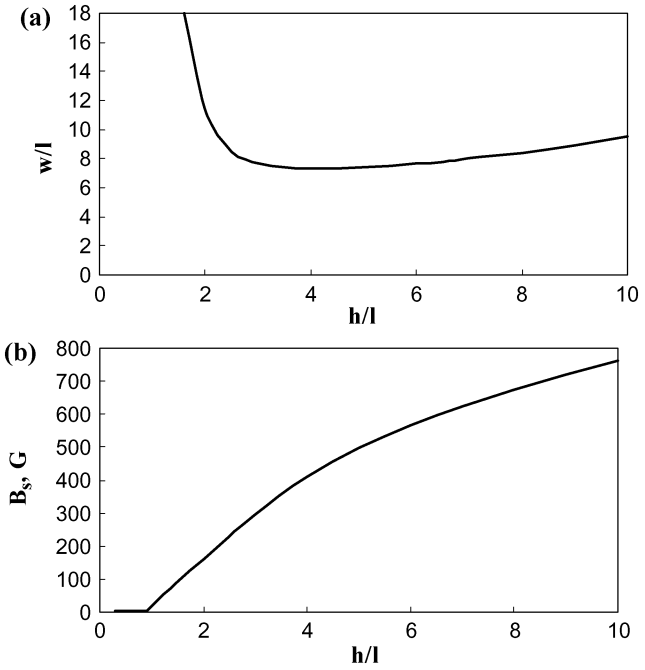

Fig. 2. Dependencies of the dimensionless stripe domain width (a) and of the saturation magnetic field (b) on the dimensionless film width.

domains existing in the sensing film and the distance between the source of the magnetic stray field and the sensing film.

The relationship between the width of the magnetic domains, the thickness of the magnetic film and the characteristic length of the magnetic material is described by the relationship

$$\frac{l}{h} = \frac{P^2}{\pi^3 h^2} \sum_{n=1}^{\infty} \frac{1}{n^3} \left[1 - \left(1 + \frac{2\pi n h}{P} \right) \exp\left(-\frac{2\pi n h}{P} \right) \right] \quad (3)$$

where P is the period of the domain structure ($P = w_1 + w_2$), where w_1 and w_2 are the widths of the domains with the up and down direction of the magnetization [10].

Typical dependencies of the domain width and the saturation field for a single-layer film on the relative thickness h/l of the film are presented in Fig. 2(a) [10]. The so-called characteristic length of uniaxially anisotropic magnetic materials $l = \sigma_w / 4\pi M_s^2$ (where σ_w is the domain wall energy density) is widely used to characterize the magnetic properties of uniaxially anisotropic magnetic films possessing a maze-like or stripe domain structure.

For the composition $(\mathrm{BiSmLu})_3\mathrm{Fe}_5\mathrm{O}_{12}$ with $4\pi M_s = 1600$ G and the uniaxial anisotropy field $H_k = 2K_u/M_s = 2000$ Oe, the characteristic length $l = \sigma_w/4\pi M_s^2 = (AKu)^{1/2}/\pi M_s^2 = 40$ nm. Here, the value of the exchange stiffness constant $A = 4 \cdot 10^{-7}$ erg/cm, and the constant of the uniaxial anisotropy $K_u = 10^5$ erg/cm^3 were used. In reality, the MPC is represented by a stack of about ten magnetostatically related thin magnetic films since they are interleaved with nonmagnetic films.

The relationship between the saturation field of the stripe domain structure existing in uniaxial magnetic films and the magnetic properties of the material was considered in [11]. A typical dependency of the saturation magnetic field for films with the above-mentioned magnetic properties on the dimensionless film thickness is presented in Fig. 2(b).

It is well known that a system of magnetostatically related films demonstrates some growth in the saturation magnetic field compared with single layer films [12]. Because in the MPC, we have two tuning parameters available, which are the thickness of the individual magnetic layers and the value of the characteristic length of the magnetic material, it is in principle possible to reduce the saturation field of the MPC structure to the level of about 10 Oe. It would be necessary to note that the minimum detectable field of the thin uniaxially anisotropic magnetic films with thickness of the order of the characteristic length of the material is restricted by the presence of coercive force. For typical iron-garnet films produced by LPE with film thickness comparable to the characteristic length of the material, the value of coercive force is near 4 Oe [13], [14].

III. Techniques Used for MPC Analysis and Common MPC Types

There are several different approaches applicable for the calculation of the multilayered systems optical properties [15]–[18]. Among them, the 4×4 transfer matrices method was proven to be an efficient and intuitively clear technique [15], [18]. That is why in this work we adopt this approach for the modeling of MPCs.

The transfer matrix for the whole structure is found as the product of the transfer matrices for each layer of MPC. The transfer matrices are determined by the layers thicknesses and their dielectric tensor. While nonmagnetic constituents of MPC can be usually regarded as isotropic media having a diagonal dielectric tensor, magnetic layers are described by the magnetization-dependent nondiagonal tensor, which is for the case of the magnetization directed along Z-axis given by

$$\hat{\varepsilon}_M = \begin{pmatrix} \varepsilon_1 & -ig & 0 \\ ig & \varepsilon_1 & 0 \\ 0 & 0 & \varepsilon_2 \end{pmatrix} \quad (4)$$

where the gyration, g, and dielectric constant, ε_2, depend on the magnetization, with g and $b = \varepsilon_2 - \varepsilon_1$ vanishing at zero magnetization. This implies that optical anisotropy for such materials is purely magnetic field-induced [1]. The gyration vector g is linear with respect to the media magnetization, while the Cotton–Mouton constant b is proportional to the magnetization squared, which classifies them as being first- and second-order magnetooptical constants, respectively. For conventional magnetooptical materials (e.g., for the yttrium iron garnets) the second-order effects can be neglected, and consequently, it is reasonably accurate to restrict our consideration here to only the first-order magnetooptical phenomena by setting the Cotton–Mouton constant, b, to zero. For the infrared-visible domain the permeability tensor $\hat{\mu}$ is considered to be a unity tensor.

The transfer matrices formalism deals with the proper modes—waves which preserve their polarization state while traveling through the media. For the isotropic dielectric proper modes are usually a set of two orthogonally polarized waves. Proper modes in the magnetic media for the electromagnetic radiation propagating parallel to the magnetization are two

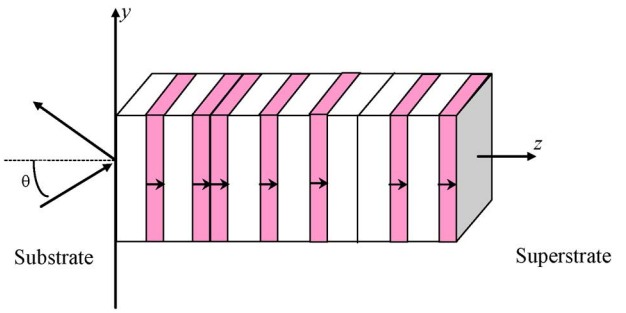

Fig. 3. Geometry of the problem. An MPC structure of type $(NM)^2(MN)^3(NM)^2$ representing a symmetric sequence of substructures containing nonmagnetic (N) and magnetic (M) layers with two defects is shown.

clockwise and counterclockwise circular polarized waves of different refractive indices:

$$n_{\pm} = \sqrt{\varepsilon_1 \pm g}. \tag{5}$$

Full characterization of the optical response of an arbitrarily structured MPC in transmission and reflection for the case of an arbitrary input polarization and the angle of light incidence is achieved by relating the wavevector components of light before and after its interaction with the structure. The details of the implementation of the transfer matrix formalism have been reported in [15] and [19].

An MPC structure is defined by a number of parameters, including the total number of layers, types and thicknesses of the layers used, types and number of layer subsequences forming the structure, and the number of defects in the local periodicity of the photonic crystal. The design space volume can be extremely large, even for the structures with a moderate total number of layers and utilising a small number of materials limited by their mutual compatibility for the selected deposition process. Structurally, the MPC designs can vary from the highly symmetric, strictly locally periodic sets of layer subsequences to the arbitrarily arranged, nonsymmetric quasi-periodic layer subsets. Three general types of MPC structure designs can be identified (shown in Fig. 3), two of which (a, b) have been investigated in some detail up to date and are commonly referred to in the literature [20], [21]. The investigation of the third (most generic) design type offers the maximum flexibility for tailoring of the spectral response of MPC structures to the requirements of practical applications, for which the efficient algorithms for the structural optimization of such structures are necessary. We have reported the initial results of the application of our MPC optimization algorithm in [22]. To generate the multiparameter-optimized designs of MPC with highly customized optical properties, we employ the computational approach based on the "exhaustive computation" technique applied to any selected subset of the overall design space defined by the chosen generic type of the structure, types of its substack constituents, and the practical restraints chosen. We then obtain the solutions representing the global optima found within the selected "cross-sections" of the multidimensional parameter space, defined by our chosen criteria.

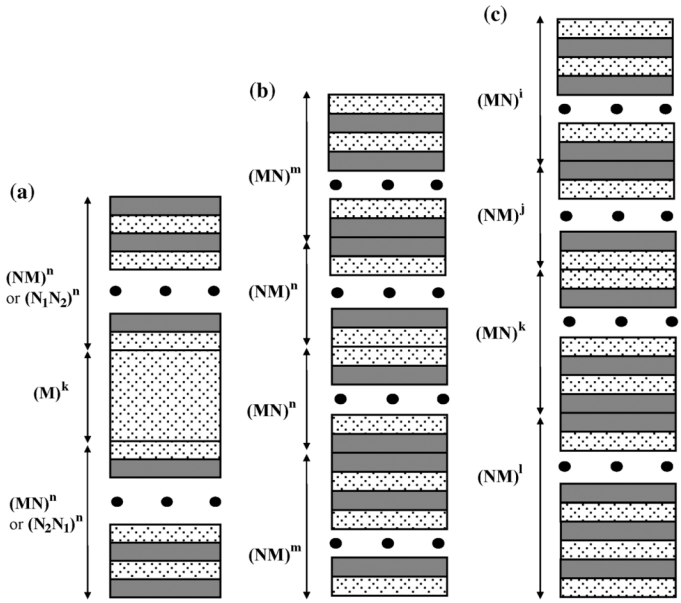

Fig. 4. Commonly used design types of MPC structures: symmetric cavity-type MPC with a thick magnetic layer surrounded by either dielectric mirrors or a sequence of magnetic (M) and nonmagnetic (N) layers (typically of quarter-wavelength optical thickness) (a); multidefect symmetric sequence of substacks typically containing a quarter-wavelength-thick magnetic and nonmagnetic layer each (b); arbitrarily sequenced (generally nonsymmetric) multidefect substacks containing magnetic and nonmagnetic layers of variable thickness with the substacks usually having a half-wave combined optical thickness (c).

It is interesting to compare the general spectral response features typically obtained by optimizing each of the MPC structural types shown in Fig. 4 with respect to the achievable Faraday rotation and power transmission. Cavity-type designs can enhance the Faraday rotation substantially whilst maintaining high levels of transmittance when the absorption is low. However, due to invoking the multipass propagation, their performance degrades very quickly with increasing absorption. Transmission spectra of optimized cavity-type MPCs usually have sharply defined resonances in both transmission and Faraday rotation, however, very strict (sub-nm) layer thickness tolerances are necessary to be achieved during the deposition in order to observe the predicted resonant peaks practically. It will also be necessary to avoid any thermooptic refractive index variations within layers in order to keep the narrow resonances at the design wavelength.

The multidefect symmetric sequences of substacks typically containing the quarter-wavelength-thick magnetic and nonmagnetic layers [Fig. 4(b)] are a class of structures offering a very high flexibility for the design of optical isolators and modulators with some degree of control over the spectral response bandwidth of such devices. This is due to their ability to generate multiple weak resonances within the complex multidefect sequences of substacks, and to overlap their spectral features in a number of ways. A great number of spectral response shapes is possible to result from the optimization of such structures. If the requirement for the symmetry of the substack repetition periods within such structures is removed, together with the usual restraint on the exact quarter-wave optical thickness of all layers, we obtain the most generic type of the structural formula [Fig. 4(c)] offering the maximum design flexibility.

During the optimization of such complex structures, the parameter space volume is reduced sequentially by first defining the types and contents of all substacks and their maximum number, and then limiting the calculations to the selected combinations of individual layer thicknesses whilst keeping the thicknesses of the elementary substack periods equal to half the design wavelength. The optimization of MPC structures is (in most cases) performed for the case of normal light incidence, and all polarization-dependent and incidence angle-dependent variations in the spectral response properties of the selected optimized designs are analyzed subsequently. At the same time, it is possible to run the optimization algorithm for the case of arbitrary angle of light incidence and arbitrary direction of the input polarization plane. The majority of optimized solutions obtained by us were found within this most generic class of quasi-periodic MPC structures, for all (or most) of the target requirements specified during the optimization.

IV. Optimization of MPC Structure for Sensor Development

A number of MPC structural types shown in Fig. 4 were evaluated computationally for their suitability for the application in reflection-mode magnetic field sensors where the absorption of LPE-deposited layers of $Bi_3Fe_5O_{12}$ is in the range of 800–1200 cm^{-1} near 560 nm. We found MPC structures of type $GGG/(M)^a(LM)^b(M)^c(ML)^d/Ag$, where the material of nonmagnetic layers L is GGG (selected for its interlayer deposition compatibility with BIG) particularly promising for the application, since the optimized structures of this type showed a good enhancement in the Faraday rotation compared to using single-layer BIG films of the same thickness as the combined thickness of the MPC magnetic components (a large MPC gain factor) whilst having a moderate total number of layers. The optimization algorithm (used in the normal incidence mode) found global optima corresponding to the maximum possible Faraday rotation in reflection per thickness of either the entire film structure, or only its magnetic constituents, by calculating the responses of all structures of the described type for a range of repetition indices $(a \ldots d)$ of $(1 \ldots 15)$ for BIG absorption coefficients ranging from 800 to 4500 cm^{-1}. The saturated gyration of BIG at 560 nm used during the calculations was $g = -0.04$, corresponding to the intrinsic Faraday rotation of $-5^\circ/\mu m$. The thickness of the reflecting layer of silver ($n_{Ag} = 0.12 + i3.44$ at 560 nm) was kept constant at 100 nm during the optimization. All optical thicknesses for layers (L, M) of the structure were kept equal to the quarter of the design wavelength (560 nm). The algorithm grouped all MPC designs from the computational domain which had reflectivity of greater than 40% at the design wavelength, Faraday rotation angles of greater than 10°, having Faraday rotation peaks within ±5 nm from the design wavelength, and limited in thickness by 30 deposition layers (or 3 μm, whichever was smaller). The number of elementary quarter-wavelength layers used in the computations (frequently referred to as the number of MPC layers in the literature) is generally larger than the number of layers that need to be deposited during the fabrication process. Then optimized designs with either the largest MPC gain factor, or the largest Faraday rotation per combined MPC thickness were obtained by filtering this preselected group. Fig. 5 shows the responses of the design optimized by maximizing the Faraday rotation angle per unit combined MPC thickness obtained with the absorption in BIG layers of 1200 cm^{-1} in reflection and Faraday rotation. The optimum design found is described by the formula $GGG/(M)^1(LM)^4(M)^2(ML)^6/Ag$ composed of only 20 layers with a combined thickness of 1.41 μm, followed by a silver coating. This MPC design was selected as a candidate for the experimental implementation of sensitivity-enhanced sensors due to having a small thickness (only 215.4 nm) in its thickest magnetic layer, which will lead to achieving the saturation of magnetization in small magnetic fields, according to Fig. 2(b).

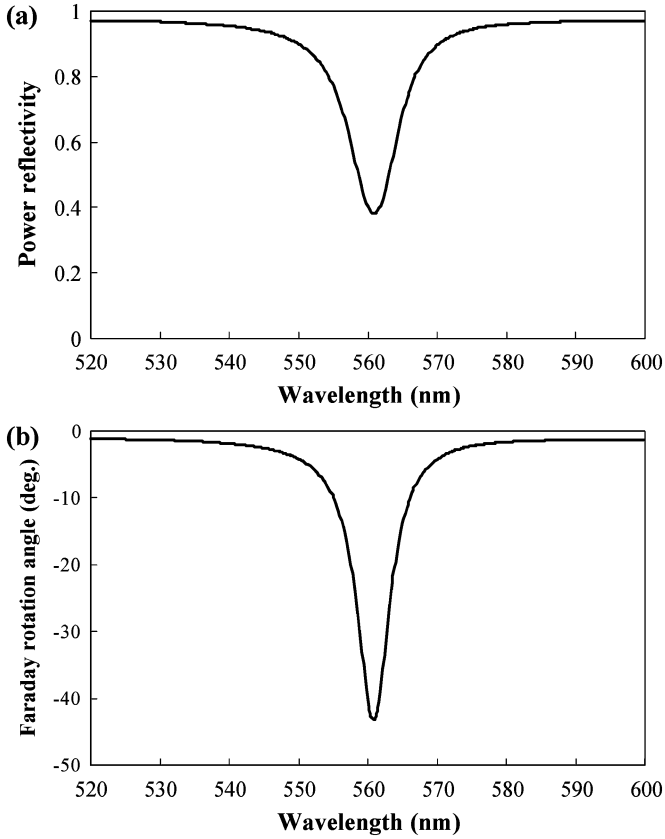

Fig. 5. Spectra of power reflectivity (a) and Faraday rotation in reflection mode (b) of an optimized sensor structure $GGG/(M)^1(LM)^4(M)^2(ML)^6/Ag$ composed of an MPC and a 100-nm-thick silver layer designed for the operation in the visible wavelength region The material of the substrate and nonmagnetic layers L is GGG ($n = 1.96$), and the material of magnetic layers M is LPE $Bi_3Fe_5O_{12}$ with $n = 2.6$, intrinsic Faraday rotation of $5^\circ/\mu m$ at 560 nm, and the absorption coefficient of 1200 cm^{-1}. The structure was optimized by selecting the design with maximised Faraday rotation in reflection per unit combined film thickness, and applying the algorithm parameters described above.

The variation in the MPC gain factor achievable by optimizing the design domain represented by the described structural type, with the value of the absorption coefficient is shown in Fig. 6. It is important to note that for all optimized designs generated by our algorithm, the MPC structure had no overall symmetry in the sequence of layers. Every parameter of the optimization algorithm (except the absorption coefficient) was kept constant during the search for the optimum designs, yet almost every optimized MPC structure found was different. This shows the importance of the application of optimization algorithm and

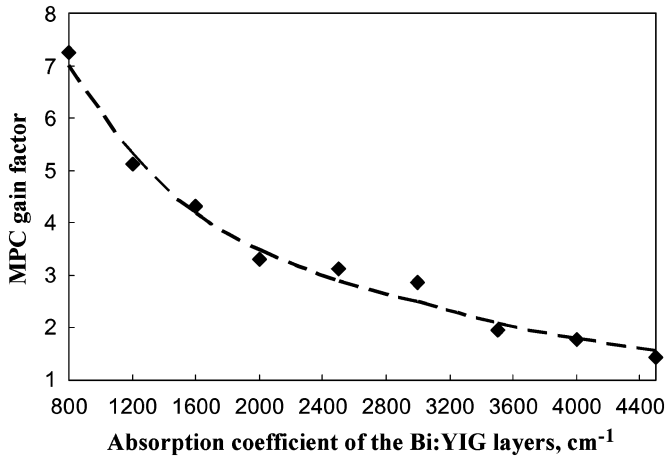

Fig. 6. Variation in the optimum MPC gain factor with the absorption coefficient of magnetic layers for optimized sensor structures of type $GGG/(M)^a(LM)^b(M)^c(ML)^d/Ag$ calculated using the optimization targets, restraints, and criteria described in the text.

using reliably measured material data during the search for the designs suitable for the practical deposition of MPC structures.

V. Conclusion

In this paper, we have considered the use of different types of 1-D MPC structures in magnetooptical visualizers and sensors. A significant increase in the device sensitivity is predicted compared with the case of single-layer MO sensing films. Using MPC structures in visualizers and sensors based on the changes in the magnetic domain structure under the influence of magnetic stray fields gives one to two orders of magnitude increase in the magnetic sensitivity of the MO sensors with a simultaneous increase in the MO sensitivity of the sensing film. The analysis taking into account the real absorbance characteristics of existing sensing films is included.

The theoretical analysis was based on the 4×4 transfer matrix formalism adapted to the search of the optimal MPC structures. A comparison of the performance of different commonly described types of MPC has been presented, with an emphasis on the optimization of MPC aimed at the possibility of the practical implementation of nano-structured sensors and on enhancing the magnetic and magnetooptical sensitivity in sensor-type applications.

References

[1] A. Zvezdin and V. Kotov, *Modern Magnetooptics and Magnetooptical Materials*. Bristol, U.K.: IOP, 1997.

[2] V. S. Gornakov, V. I. Nikitenko, L. H. Bennett, H. J. Brown, M. J. Donahue, W. F. Egelhoff, R. D. McMichael, and A. J. Shapiro, "Experimental study of magnetization reversal process in nonsymmetric spin valve," *J. Appl. Phys.*, vol. 81, p. 5215, 1997.

[3] M. Shamonin, M. Klank, O. Hagedorn, and H. Dotsch, "Magneto-optical visualization of metal-loss defects in a ferromagnetic plate: Experimental verification of theoretical modeling," *Appl. Opt.*, vol. 40, pp. 3182–3189, 2001.

[4] M. Klank, O. Hagedorn, M. Shamonin, and H. Dotsch, "Sensitive magneto-optical sensors for visualization of magnetic fields using garnet films of specific orientation," *J. Appl. Phys.*, vol. 92, pp. 6484–6488, 2002.

[5] R. D. Shull, E. Quandt, A. T. Shapiro, S. Glasmachers, and M. Wuttig, "Magneto-optic indicator film observations of domain motion in magnetostrictive materials under stress," *J. Appl. Phys.*, vol. 95, pp. 6948–6950, 2004.

[6] D. Giller, B. Kalisky, A. Shaulov, T. Tamegai, and Y. Yeshurun, "Magneto-optical imaging of transient vortex states in superconductors," *J. Appl. Phys.*, vol. 89, pp. 7481–7483, 2001.

[7] K. B. Rochford, A. H. Rose, M. N. Deeter, and G. W. Day, "Faraday effect current sensor with improved sensitivity-bandwidth product," *Opt. Lett.*, vol. 19, pp. 1903–1905.

[8] M. J. Steel, M. Levy, and R. M. Osgood, Jr., "Large magneto-optical kerr rotation with high reflectivity from photonic band gap structures with defects," *J. Lightw. Technol.*, vol. 18, pp. 1289–1296, 2000.

[9] H. Kato and M. Inoue, "Reflection-mode operation of one-dimensional magneto-photonic crystals for uses in film-based magneto-optical isolator devices," *J. Appl. Phys.*, vol. 91, pp. 7017–7019, 2002.

[10] C. Kooy and U. Enz, "Experimental and theoretical study of the domain configuration in thin layers of $BaFe_{12}O_{19}$," *Philips Res. Rep.*, vol. 15, pp. 7–16, 1960.

[11] J. A. Cape and G. W. Lehman, "Magnetic domain structures in thin uniaxial plates with perpendicular easy axis," *J. Appl. Phys.*, vol. 42, pp. 5732–5756, 1971.

[12] Y. S. Lin, P. J. Grundy, and E. A. Giess, "Bubble domains in magnetostatically coupled garnet films," *Appl. Phys. Lett.*, vol. 23, pp. 485–488, 1973.

[13] V. A. Kotov, D. E. Balabanov, S. M. Grigorovich, V. I. Kozlov, and V. K. Nevolin, "Magnetic and magnetooptical properties of the transition layer in epitaxial bismuth-galium iron garnet structures," *Sov. Phys. Tech. Phys.*, vol. 31, pp. 544–549, 1986.

[14] V. I. Burkov, D. E. Balabanov, V. A. Kotov, and G. S. Semin, "Uniaxial magnetic anisotropy and magnetic circular dichroism spectra of ultra thin iron garnet films," *Sov. Phys. Tech. Phys.*, vol. 31, pp. 1245–1249, 1986.

[15] V. I. Belotelov and A. K. Zvezdin, "Magneto-optical properties of photonic crystals," *J. Opt. Soc. Amer. B*, vol. 22, no. 1, p. 286, 2005.

[16] K. Sakoda, *Optical Properties of Photonic Crystals*. New York: Springer, 2001.

[17] A. Yariv and P. Yeh, *Optical Waves in Crystals: Propagation and Control of Laser Radiation*. New York: Wiley, 1983, p. 608.

[18] S. Visnovsky, "Theory of magneto-optical effects in magnetic multilayers," *J. Magn. Soc. Jpn.*, vol. 15, Suppl. S1, pp. 67–72, 1991.

[19] M. Vasiliev, V. I. Belotelov, A. N. Kalish, V. A. Kotov, A. K. Zvezdin, and K. Alameh, "Effect of oblique light incidence on magnetooptical properties of one-dimensional photonic crystals," *IEEE Trans. Magn.*, vol. 42, no. 3, pp. 382–388, Mar. 2006.

[20] M. Levy, H. C. Yang, M. J. Steel, and J. Fujita, "Flat-top response in one-dimensional magnetic photonic bandgap structures with faraday rotation enhancement," *J. Lightw. Technol.*, vol. 19, no. 12, pp. 1964–1969, Dec. 2001.

[21] S. Sakaguchi and N. Sugimoto, "Transmission properties of multilayer films composed of magneto-optical and dielectric materials," *J. Lightw. Technol.*, vol. 17, no. 6, pp. 1087–1092, Jun 1999.

[22] M. Vasiliev, K. Alameh, V. Belotelov, V. A. Kotov, and A. K. Zvezdin, "Magnetic photonic crystals: 1-D optimization and applications for the integrated optics devices," *J. Lightw. Technol.*, vol. 24, no. 5, pp. 2156–2162, May 2006.

Manuscript received November 9, 2007; revised November 27, 2007. Corresponding author: M. Vasiliev (e-mail: m.vasiliev@ecu.edu.au).